# 1

# CLIMATE & ENVIRONMENTAL MODELLING

Capacity to model and forecast climate and environmental processes at different spatio-temporal scales has the potential to revolutionize our approach and ability to address many issues that concern us closely. It was to address these issues in an integrated manner and to generate a capability for multiscale forecasting that CEMP was initiated.

## *Inside*

# A: Climate Variability, Climate Change and Sustainability

## A.1 Orthogonal Components of the Indian Summer Monsoon: Structural and Epochal Changes

The Indian Summer Monsoon (ISM) rainfall and its interannual variability determine the agricultural prospects of the nation. A clear understanding of the interannual variability of ISM is still lacking, as reflected in poor skill of prediction even by the most recent models. One issue that has not been examined well is whether the rainfall events that build up ISM form a continuum in terms of their intensity and distribution. Estimation of such a rainfall requires quantitative delineation of the component of rainfall from large-scale forcing from that due to local and synoptic variability. A natural partitioning, however, is possible because the rainfall events that build up the ISM do not all behave coherently, but belong to distinct classes (categories) with independent spatio-temporal distribution. In terms of absolute intensity (that is without reference to local climatology), most rain events during ISM are below 5 cm/day (weak rain events, hereafter WRE), as shown by distribution of number of events in different categories (Figure 1.1).

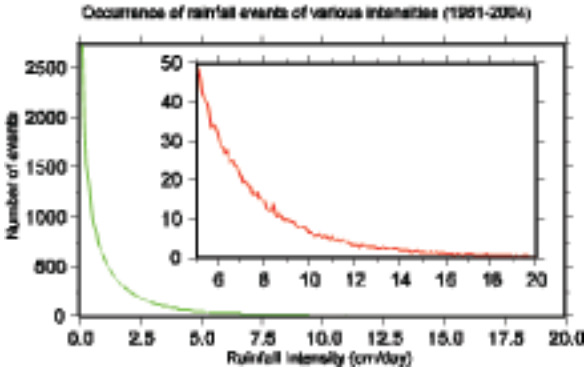


Figure 1.1 Occurrence of rainfall events of different intensities averaged over the years 1951 - 2004 based on daily gridded (1°X1°) data from Indian meteorological department, India. The x-axis represents intensity of rainfall events normalized to the respective maximum (20 cm).The y axis shows number of rain events in a given category during June-September over India. It may be seen that the number of events falls sharply upto about 5 cm/day (outer panel) and then remains more or less constant (inset panel).

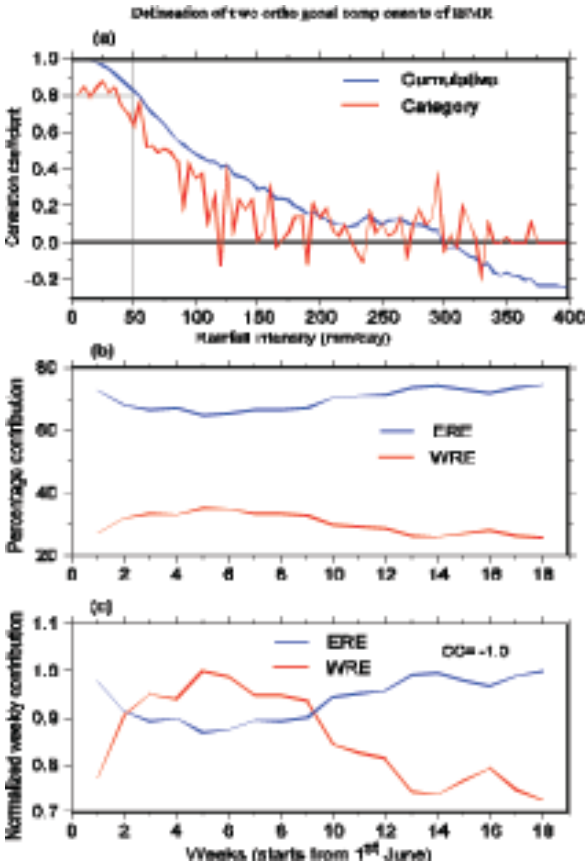


Figure 1.2 (a) Correlation coefficient (CC) between all-India seasonal rainfall and seasonal rainfall at different categories (red line) and cumulative seasonal rainfall at different categories (blue line) for the period (1951-2004) based on IMD data. (b) Seasonal cycle of percentage contribution (PC) from ERE events (red line) and WRE (blue line) to the total seasonal rainfall (c) Seasonal cycle of ERE and WRE normalized to respective weekly maximum of PC. The correlation coefficient between weekly rainfall from ERE and WRE is given in the bottom panel.

To objectively separate the ERE from the other component of ISM rainfall we have examined inter category correlation coefficients in area-averaged daily rainfall. The correlation coefficients clearly show (Figure 1.2a) the high inter category correlation until about 5 cm/day followed by a sharp drop. In our description, therefore, the events with intensities lower than 5 cm/day form a class (Weak rain events or WRE) from those with Extreme Rain Events (ERE).

The distinct structures of the seasonal cycles of ERE and WRE components come out clearly when each is plotted normalized to its own (weekly) maximum (Figure 1.2b), while ERE seasonal cycle begins with a low (~ 75% of the maximum) value in June and attains its maximum in July, the WRE seasonal cycle begins with near maximum in early June and attains its minimum value (~90%) of the maximum) in July. On the other hand, the seasonal cycle due to ERE falls sharply beyond the tenth week, while the WRE seasonal cycle maintains near maximum value until the end of the season. The characteristic seasonal cycle of ISM, therefore, is a combination of these two distinct and compensating seasonal cycles.

This analysis provides a new mechanism for understanding variability of Indian summer Monsoon.

*K V Ramesh and P Goswami*

## A.2 Indian Summer Monsoon in Future Climate Projection by a High Resolution Global Model

The impact of climate change on the Indian summer monsoon has been investigated using a super high-resolution global general circulation model. The model with approximately 20-km mesh horizontal resolution can resolve features on finer spatial scales, which were till now resolved by employing high-resolution regional models. This in turn leads to better representation of local physics (such as land surface, boundary layer, cloud and deep convection characterizations). In addition, regional models are known to have high dependency on the lateral boundary forcing and significant inability to represent regional-global scale interactions comprehensively. Another advantage of this 20-km global model is its fidelity in representing the regional distribution of the present-day monsoon rainfall (Figure.1.3).

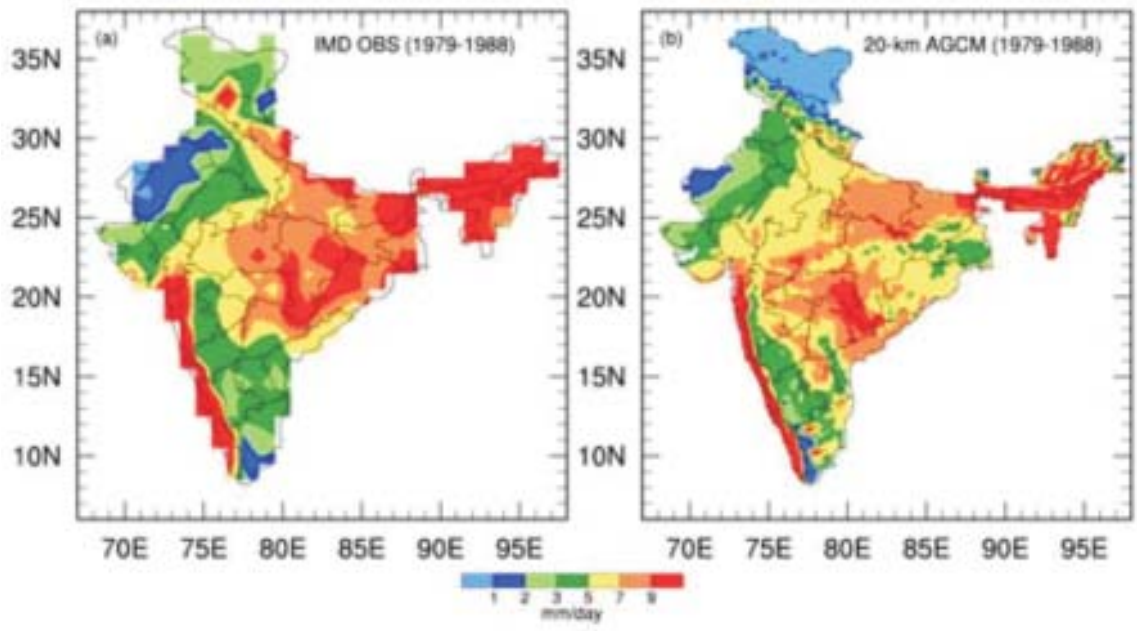


Figure 1.3 JJAS mean rainfall from IMD observation (a) and present-day simulation of the 20-km model (b).

The super high-resolution future scenario (2075-2084) for the Indian summer monsoon (Figure 1.4), shows widespread but spatially varying increase in rainfall over the interior regions and significant reduction in orographic

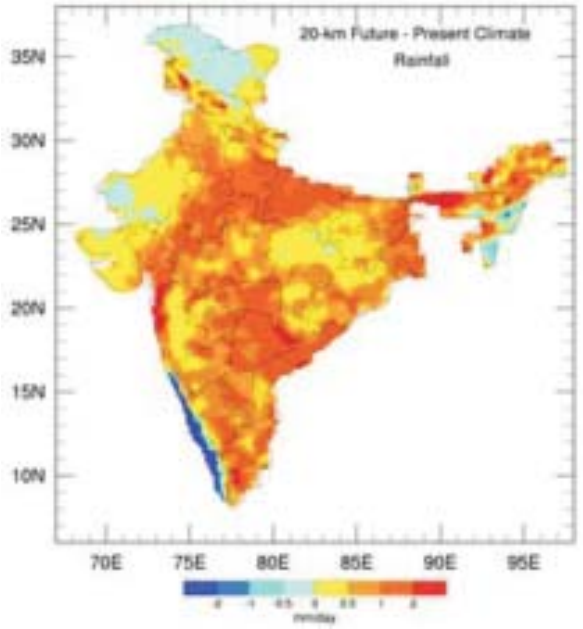


Figure 1.4 JJAS mean difference in rainfall between future projection (2075-2084) and present-day (1979-1988) simulation of the 20-km model. Differences significant at 95% level are stippled.

rainfall over the west coasts of Kerala and Karnataka and the eastern hilly regions around Assam. Over these regions, the drastic reduction of wind by steep orography predominates over the moisture build-up effect (that causes enhanced rainfall over other parts) in reducing the rainfall. This indicates that monsoon rainfall is strongly controlled by parameterized physics and high-resolution processes which need to be resolved with adequately high resolution.

The model projects substantial, spatially heterogeneous increase in both extreme hot and heavy rainfall events over most parts of India by the end of the century (Figure 1.5). While fine-scale surface moisture feedbacks influence the response of extreme hot events, extreme precipitation is influenced by fine-scale

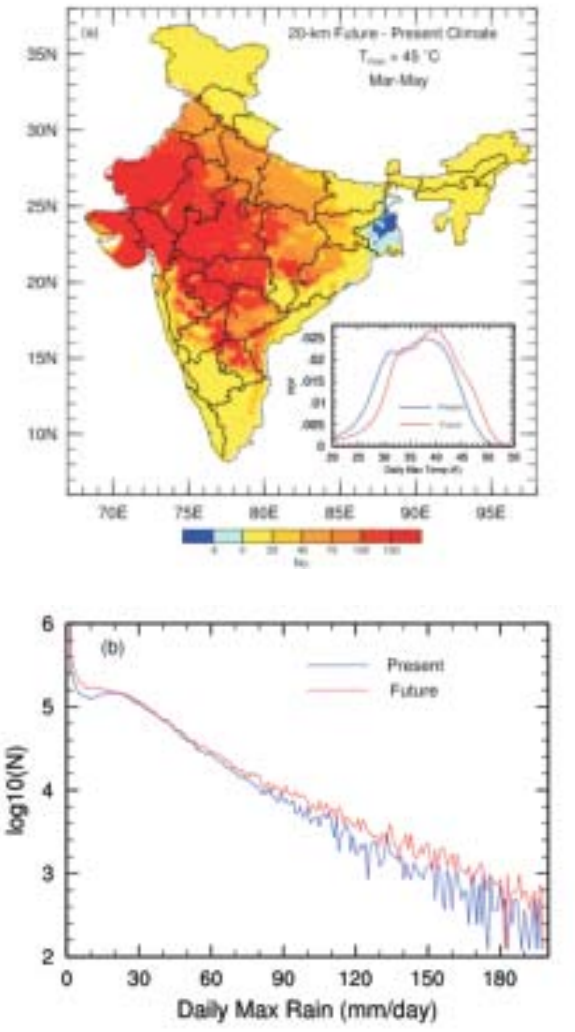


Figure 1.5 Difference in the number of days with maximum temperature greater than (a) 45°C in March-May and (b) frequency distribution of daily maximum precipitation over India during June-September between the future climate (2075-2084) and present day (1979-1988) climate simulation.

orography, evaporation, moisture content and circulation. Thus, the results indicate that consideration of fine-scale processes is critical for accurate assessment of local and regional-scale vulnerability to climate change.

*K Rajendran & A Kitoh*

## A.3 Simulation of Intraseasonal Variability in a High Resolution Global Model.

This study documents the detailed characteristics of the tropical intraseasonal

variability (TISV) in the MRI-20km60L AGCM that uses a variant of the Arakawa-Schubert cumulus parameterization. Mean states, power spectra, propagation features, leading EOF modes, horizontal and vertical structures, and seasonality associated with the TISV are analyzed. Results show that the model reproduces the mean states in winds realistically and in convection comparable to that of the observations. However, the simulated TISV is less realistic. Power spectra and lag correlation of the signals do not propagate dominantly either in the eastward direction during boreal winter or in the northward direction during boreal summer. A combined EOF (CEOF) analysis shows that winds and convection have a loose coupling that cannot sustain the simulated TISV as realistically as that observed. The less realistic TISV suggests that the representation of cumulus convection needs to be improved in this model.

*P Liu, Y Kajikawa, B Wang, A Kitoh, T Yasunari, T Li, H Annamalai, X Fu, K Kikuchi, R Mizuta, K Rajendran, D E Waliser and D Kim*

## A.4 Regional Aerosol Direct Radiative Forcing Impact on Indian Summer Monsoon Precipitation: A General Circulation Model Study

The aerosols affect climate directly by reflecting and absorbing solar radiation, and to a lesser extent through absorption and emission of longwave radiation. The chemical composition and size distribution of aerosols effectively characterize their optical properties. The physical properties of aerosols are strong functions of their sources, which are widely distributed and highly variable from one region to the other. Thus, the aerosol impact on climate system has a strong regional component. The effect of regional aerosols over India where the emission of aerosol precursors has been rapidly increasing during the last decades and is expected to continue to increase for the coming decades as a result of the economic development of the region, can be a significant influential factor for Indian summer monsoon. In this study, the relative roles of scattering and absorbing aerosols, and their combined effect on Indian summer monsoon are assessed using the NCAR community atmospheric model (CAM) at T42 horizontal resolution with 31 vertical levels.

In general, direct radiative forcing leads to large-scale suppression of continental monsoon rainfall over India and overall enhancement of rainfall over adjacent oceans (Figure 1.6). But, significant local and remote impacts due to regional aerosols are evident

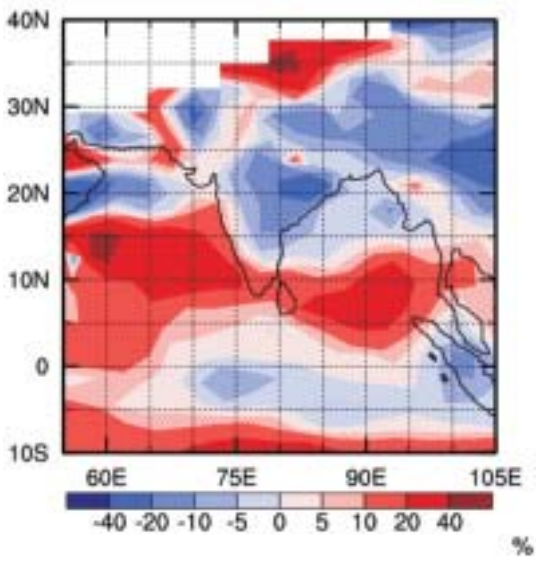


Figure 1.6 Climatological summer (June-September) mean rainfall difference between simulations with and without aerosols as percentage of the climatological summer mean rainfall from the simulation without aerosol.

once realistic aerosols are prescribed over the Indian region. While local impact appears through land surface cooling, remote impact is through changed heating induced modulations in global circulation. Incorporating as much realistic aerosol properties as possible is an important factor in assessing impacts.

*Sajani Surendran and K Rajendran*

## A.5 Measurements of Greenhouse gases (GHG) in India

The rapidly expanding economies of East Asia are showing a swift increase in GHG emissions. From 1993 to 2003 $CO_2$ emissions from India have increased by 57 percent and such a trend will likely continue though per capita emissions still lag far behind those of Europe and the US. The development of the Indian sub-continent with a population of ~1.2 billion, may lead to significant changes in the regional distribution of GHGs in the atmosphere. Such development emphasizes the urgent need for initiating a long term monitoring of the greenhouse gas concentrations over the Indian subcontinent.


Figure 1.7 Port Blair site in Andaman.

As part of the Indo-French collaboration stations at Hanle and Pondicherry have been set up with the help of IIA for measuring GHG concentrations. In continuation a continuous monitoring station for $CO_2$ and $CH_4$ at Port Blair in Andamans is planned. A team from the project, sanctioned by CSIR for setting up the station at Andamans, visited Port Blair for identification of the site. Port Blair is in the South Andaman region as shown in Figure 1.7. Air sampling has started at the site chosen for this work at Port Blair near the coast as seen in the Figure 1.8.

Figure1.8 Air sampling at Port Blair using 1 lt glass flasks for collection of air.

**Quantitative Network Design (QND):**

Top-down approaches convert the spatial and temporal gradients of atmospheric concentrations of greenhouse gases into space and time varying sources and sinks. However, the poor density of the monitoring of greenhouse gases over some continents leads to large uncertainties in the regional flux estimates based on atmospheric inversions.

In this work, the methodology and the results of a network design study to determine the optimal network for monitoring $CO_2$ in India is presented. The approach is based on a genetic algorithm. Optimality is defined with several criteria, among which are error reduction for specific regions in India, for the whole country or for a larger zone including other neighbouring countries. A special focus is given on the location of measurement stations, and several scenarios are tested, based on possible locations in terms of infrastructure, staff and energy.

Genetic algorithms are used to minimize complex non-linear functions, in this case posterior uncertainty, as a function of station locations (Rayner et al., 2004). The algorithm maintains a population of potential solutions. Each "solution" is a list of stations. In each iteration members of the population can : exchange parameter values (breed), incur small random changes (mutate), compete according to their fitness (culling), be cloned to refill population after culling. Minimization is performed for the posterior uncertainty of a region (e.g. India) or a group of regions (e.g. South Asia).

A modelling experiment has been performed to infer the best GHG measurement network in India. " Best " is defined by the minimisation of the residual uncertainty of $CO_2$ surface net fluxes as inferred by an atmospheric inversion. Atmospheric response functions calculated with the LMDZt transport model (1°x1° zoom over India) were included in a cyclostationary synthesis inversion that was coupled to a genetic algorithm. A posteriori uncertainties only depend on the response functions and on a-priori uncertainties on the fluxes and of the observations (Gloor et al., 2000, Rayner et al., 2004). The genetic algorithm drives a series of inversions in order to determine iteratively the locations minimizing the aposteriori uncertainty over a given region (from global to India). The locations of 63 existing stations were imposed and, the number of additional stations was varied from 1 to 10.

In the finer scale model of sources, India is divided into 7 regions in contrast to the earlier work with the TRANSCOM protocol where all of India and China were clubbed into a single Temperate Asia region. The existing network of stations is shown in the Figure 1.9. Adding 5 stations, with a constraint to minimize annual uncertainty over India, a location in the Bay of Bengal is picked up as shown in the Figure 1.10.

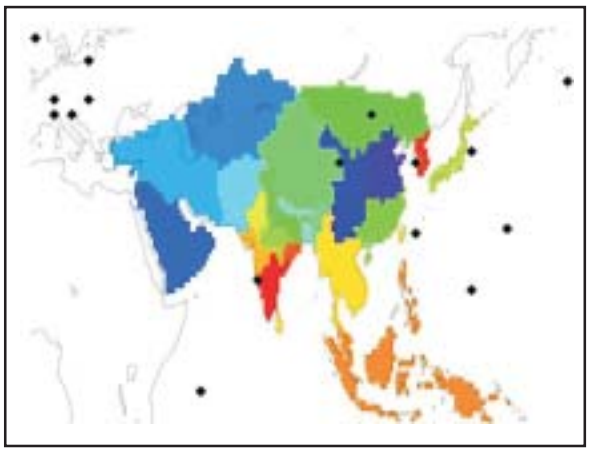

Figure1.9 Existing Network of Stations.

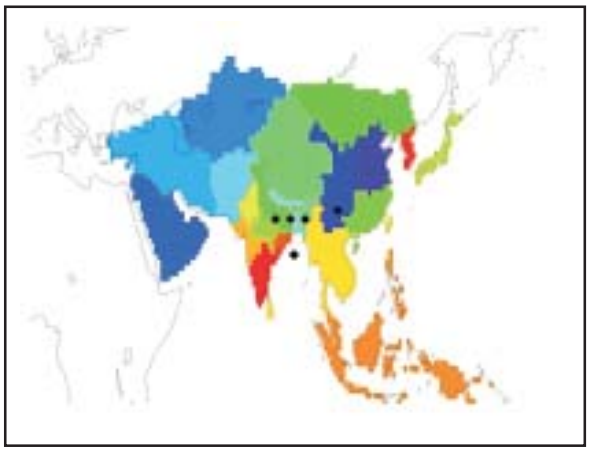

Figure1.10 Additional five stations.

Figure1.11 Adding ten stations.

Adding ten stations, locations downward (during the summer monsoon) of the main

source regions in India are picked up by the genetic algorithm as shown in the Figure 1.11.

This study has shown the potential of QND for optimal selection of GHG measurement stations and will form the basis for future site selection.

*N K Indira, P S Swathi, B C Bhatt, R Kirubagaran, V K Gaur, M Ramonet, P Rayner, P Bousquet*

## A.6 Parameter Sensitivity Analysis for the Coupled Physical-Biological Model in the Indian Ocean

A central problem in large-scale biogeochemical modeling is determining how well the coupled physical-biological-chemical models can simulate observed variability of various biogeochemical components in different ocean environments. The main objective in biogeochemical modelling studies is the identification of key biogeochemical elements and processes, estimation of the model parameters and role of biology on the carbon flux between ocean and atmosphere at different spatial and temporal scales. Detailed analysis of the biological fluxes which influence the carbon chemistry in the ocean for different parameter values are done at C-MMACS using a 3D coupled physical-biological-chemical model of the oceanic carbon cycle. The marine ecosystem model and carbon chemistry model are evaluated by using U.S. JGOFS data, BOBPS data, WOCE data, satellite data and buoy data for different values of a few of the parameters which influence the regeneration of ammonium and growth of zooplankton and hence the carbon flux across the air-sea interface. The results of the study clearly illustrate the importance of (a) control by zooplankton grazing and (b) regeneration of ammonium in controlling the ecosystem dynamics of the Arabian Sea (AS) and the Bay of Bengal (BOB). The set of ecosystem parameters which has great potential for application for further studying the marine productivity and carbon dioxide transfer in the Indian Ocean have been isolated in this study. A manuscript has been submitted on this study and is accepted for publication.

In these simulations, spatial and temporal variations of all the state variables, Primary Productivity (PP), Partial Pressure of carbon dioxide at the sea surface (pCO2), Carbon Flux across the air-sea interface, and the fluxes between the state variables are examined in detail for AS and BOB for four numerical

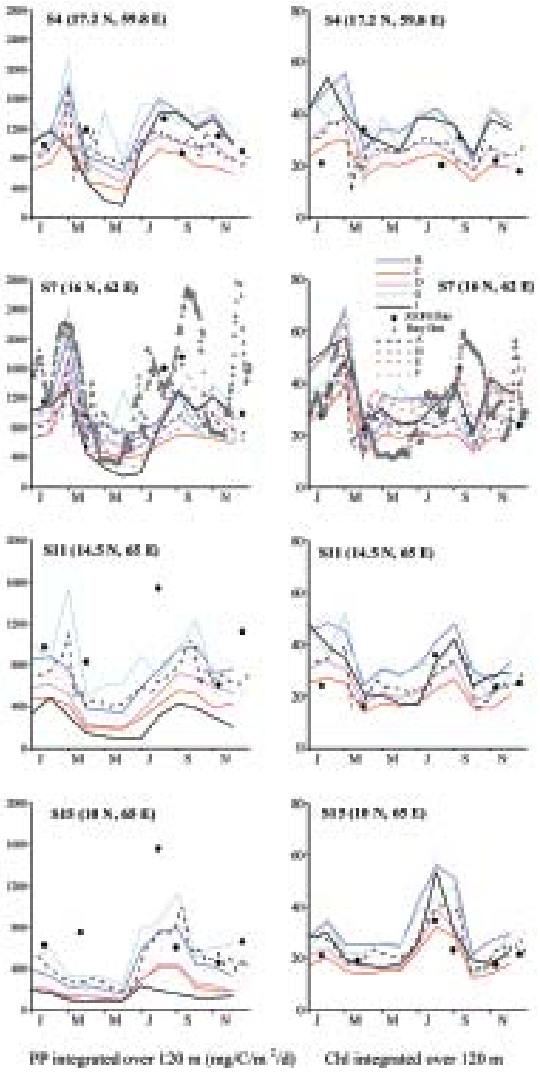

Figure1.12 Seasonal variation of Primary Productivity integrated over 120m (mg C/m2/day) and Chlorophyll integrated over 120m (mg Chl/m2) obtained from nine numerical simulations (solid lines) compared with US JGOFS cruise data (dots) at four stations S4, S7, S11 and S15 and buoy data at S7 in Arabian Sea.

experiments to understand the effect of parameters on the air-sea carbon flux. The seasonal variation is studied by considering averages in four seasons, namely, South West Monsoon (June, July & August, SWM), North East Monsoon (December, January & February, NEM), Spring Inter Monsoon (March, April & May, SIM) and Fall Inter Monsoon (September, October & November, FIM).

We focus on specific sites occupied by JGOFS and the WHOI buoy (time series) to study the temporal variability in greater detail. Figure 1.12 shows the seasonal variation of monthly averages of depth integrated Primary Productivity (left panels) and Chlorophyll (right panels) obtained from nine model simulations compared with the snapshots of JGOFS cruise data at S4, S7, S11 and S15 (Note the sites are increasingly offshore from the Oman coast), and with data obtained from buoy located at a station near S7 in Arabian Sea. At S4 and S7, one of the numerical experiments (exp I) is close to US JGOFS cruise data. At S11, three of the numerical, namely, experiments A, F and G are close to JGOFS data during all seasons except during August-September. At S15, all model simulations underestimate Primary Productivity during January, March and August. At S7, monthly average values of depth integrated Primary Productivity are also compared with the daily average values of depth integrated Primary Productivity obtained from buoy data (Marra et al). Many of the numerical simulations could capture the bloom observed in buoy data during February-March. Another feature that can be seen is the decrease in depth integrated primary productivity as we go offshore (from S4 to S15) from the Oman coast. Between the simulation experiments, exp I seems to be the lowest in PP and exp G is the highest. The range between exp I and G can be qualitatively explained by (a) the reduction of ammonium due to lower regeneration in exp I and (b) reduced grazing by zooplankton in exp G.

Depth integrated Chlorophyll is compared with the snapshots of JGOFS cruise data in the right panels of Figure1.12. The experiments are generally spread on either side of the observations. The blooms during North East Monsoon and South West Monsoon as well as low Chlorophyll during Spring Inter Monsoon are captured by all simulations. At S7, many of the numerical simulations capture the bloom observed during February-March.

The profiles of nitrate (Nn) from all the experiments are compared with JGOFS data during six times over a year at stations S4 and S7 in Figure 1.13. Nitrate concentrations in the upper ocean obtained from many of the simulations agree well with the observed data during all seasons and at both stations. Nitrate concentration below 100m is influenced by the remineralization and nitrification processes. More studies are required to be done on modeling of re-meineralization processes below the euphotic zone.

A new marine ecosystem model having a variable Carbon: Nitrogen Ratio for different components of the ecosystem, detailed representation of Dissolved Organic Matter (DOM) with dynamic C/N, Nitrogen fixation and Calcification is incorporated into MOM4 (recent version of OGCM). Several model simulations have been carried out by changing the values of a few parameters and some of the processes. Results of these model simulations are being evaluated using cruise data and satellite data.

Marine Ecosystem Models with different micro and macro nutrients are being studied to formulate the uptake kinetics of iron, silica and phosphorus by phytoplankton. This new marine ecosystem model will be incorporated in the

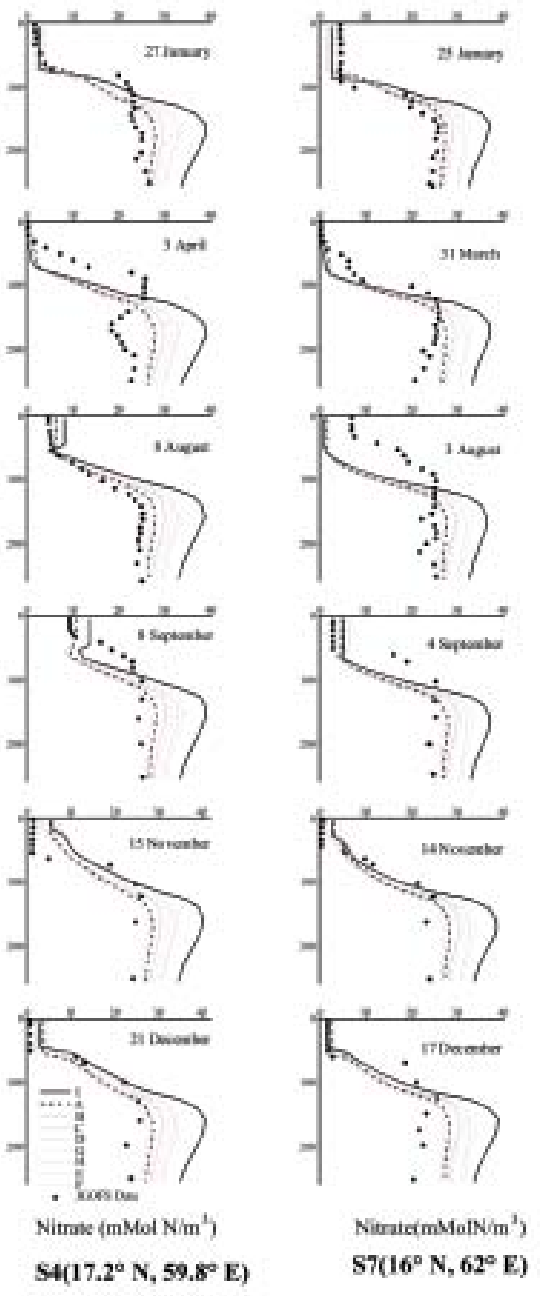


Figure1.13 Profiles of Nitrate (m Mol N/m3) obtained from nine numerical simulations (solid lines) compared with US JGOFS cruise data (dots) during six times over a year at S4 and S7 in Arabian Sea.

1D and 3D physical oceanographic models to study the effect of iron fertilization on the carbon flux across the air-sea interface, in the Indian Ocean and the Southern Ocean.

*M K Sharada, P S Swathi, K S Yajnik and C K Devasena*

# B: Forecast and Analysis of Indian Summer Monsoon

## B.1 C-MMACS Long-range, High-resolution Forecast of Summer Monsoon, 2008

It has been long realized that advance and high-resolution forecasting of monsoon was critical if the Indian economy was to be insulated from the vagaries of monsoon. At the same time, it became clear that with the advance in numerical modeling and HPC, dynamical models provided not only acceptable but also a feasible solution for advance, high-resolution forecasting of monsoon rainfall. Realizing that India (in 2001) didn't have a functional platform for dynamical forecast of monsoon more than a month in advance, C-MMACS initiated an effort to develop a platform for forecasting monsoon rainfall at long-range (1-3 months) and high spatial resolution.

C-MMACS effort was pioneering in India, and ran opposite to several firmly held notions. It had therefore, become necessary to show the effectiveness of the methodology in a most objective and transparent manner. To this end, C-MMACS had started issuing its (experimental) monsoon forecasts well before

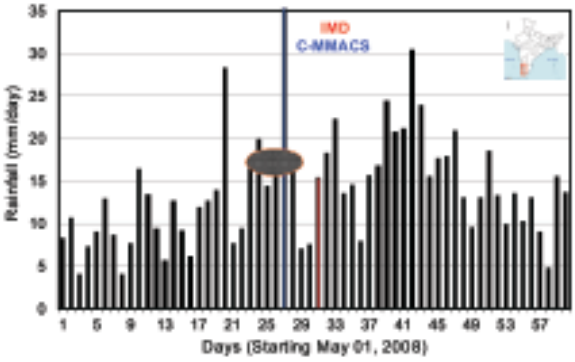


Figue 1.14 Area-averaged daily rainfall from C-MMACS forecasts for May-June 2008. The simulation is an ensemble average of five initial conditions between April 01 and May 01 from NCEP Re-analysis. The result is over the onset domain (75-77E, 8-12N). The date of onset of monsoon predicted by the model (27th May) and IMD announced (31st May) are marked with blue and red bars respectively.

the season for a most objective and post forecast evaluation. C-MMACS followed this procedure since 2003.

In 2005, IMD took the constructive step of assimilating these forecasts to its own; and theC-MMACS forecasts are provided to IMD as a part of this national exercise. In addition to IMD, the C-MMACS forecasts are also sought and used by other agencies like the Govt. of Karnataka (KSNDMC).

### Forecast of Date of Onset

The C-MMACS forecast of an early onset was realized only partially. The date of onset of monsoon (DOM) according to the criteria of sustained, significant and large-scale rainfall in C-MMACS forecast was May 27, 2008 (Figure 1.14). The announced DOM according to IMD is May 31, 2008, essentially coincidental with the next significant peak in forecast.

### Forecast of Monthly and Seasonal Anomalies

The forecasts of monthly anomalies are made by first calculating anomalies with respect to the 25-year model mean for each member of the ensemble. The ensemble average is then determined as an average over the ensemble with equal weight. The monthly rainfall anomalies are expressed as percentage of the model mean.

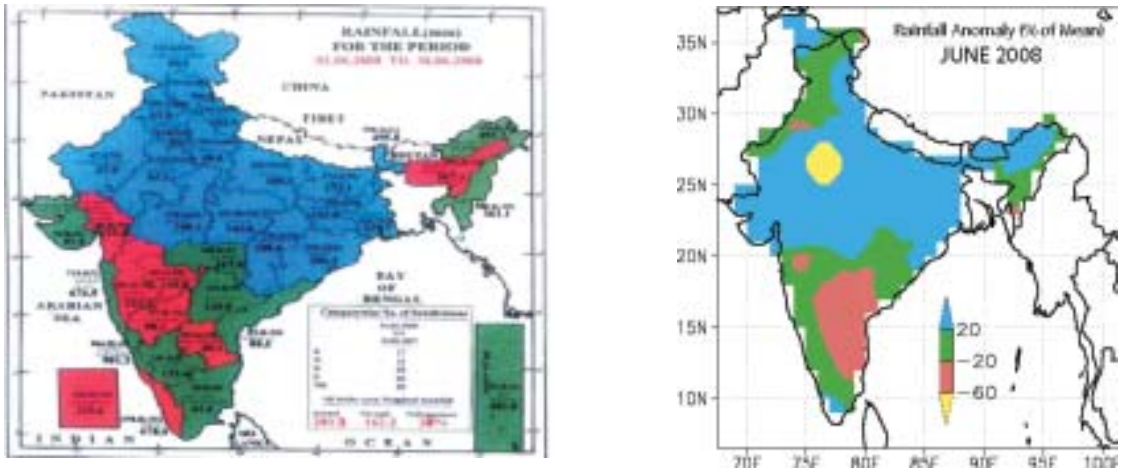


Figue1.15 Comparison of spatial distribution of monthly rainfall categories in observation (IMD) and model forecast (C-MMACS) for June, 2008.

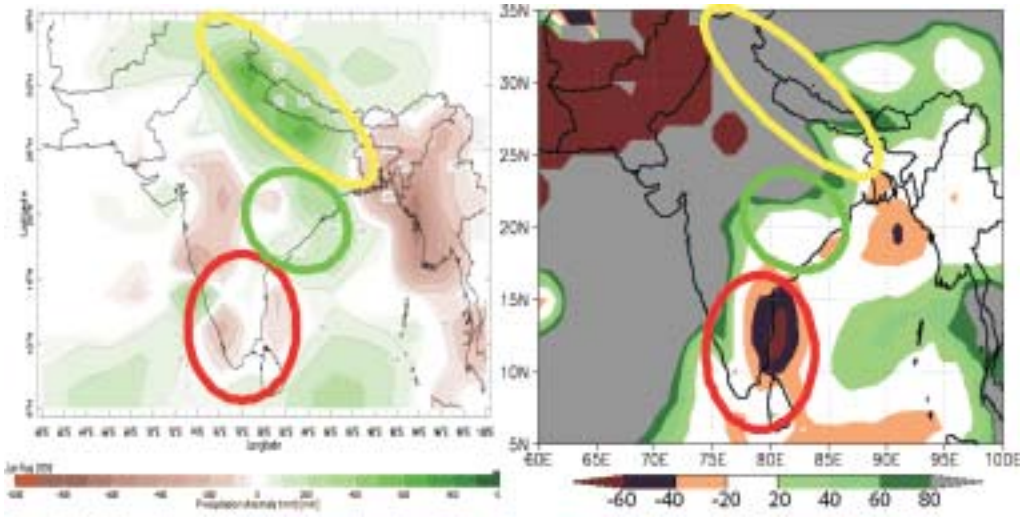


Figue1.16 Comparison of distribution of rainfall anomalies of (JJA) 2008 from NOAA analysis ( top panel) and C-MMACS long range forecasting (bellow panel)

Distribution of anomalies in the monthly rainfall of June, 2008 from IMD observation (www.imd.ernet.in, left panel) and C-MMACS long range forecasting (right panel) are presented in Figure 1.15.

The distribution of anomalies including ocean part in the seasonal rainfall of (JJA) 2008 from NOAA CAMS Analysis (left panel) and C-MMACS long range forecasting (right panel) are presented in Figure 1.16.

*K C Gouda and P Goswami*

## B.2 Comparative Evaluation of two Ensembles for Long-range Forecasting of Monsoon Rainfall

It is now well known that changes in initial conditions can give rise to substantial changes in the forecasts even at long range. Ensemble averaging of forecasts from different initial conditions provides an efficient way of assessing and reducing uncertainties in the forecasts due to inherent uncertainties in the initial conditions. However, the procedure for generating the ensemble of forecasts has to be based on careful consideration. Although there now exist several and well tested frameworks for ensemble forecasting at short range, procedure for and impact of ensemble forecasting on long-range forecasting of monsoon remains relatively less explored. In particular, the procedure for choice of the ensemble for long-range forecasting of monsoon needs special consideration. The Indian summer monsoon is characterized by a number of intraseasonal oscillations (ISO) whose phases and amplitudes can significantly affect the monsoon forecast and which can be adequately sampled only using initial states spread over time scales comparable to characteristic time scales of these ISO.It has been shown that use of initial states spread over a longer period (such as April 01-May 01) results in better ensemble average for long-range forecasting of Indian summer monsoon than that from an ensemble of closely packed states with shorter lead. An optimized configuration for long-range forecasting of monsoon using a variable resolution general circulation model has been adopted. Climatological monthly mean SST field is used to assess realizable skill, as use of observed SST provides only potential skill. Comparison of 5-members wide-lead (April 01-May 01) ensemble average forecasts with 5-member compact-lead (April 27-May 01) ensemble average forecasts for 24 (1980-2003) hindcasts has been made; it is shown that the skill of the wide-lead ensemble average is superior to that of the compact-lead ensemble at different spatial and temporal scales in spite of the longer lead of the former. The climatological seasonal cycle (June-August) of area-averaged daily rainfall (Figure 1.17) compares well for WL with the corresponding seasonal cycle from IMD data (Figure 1.17, thick line).

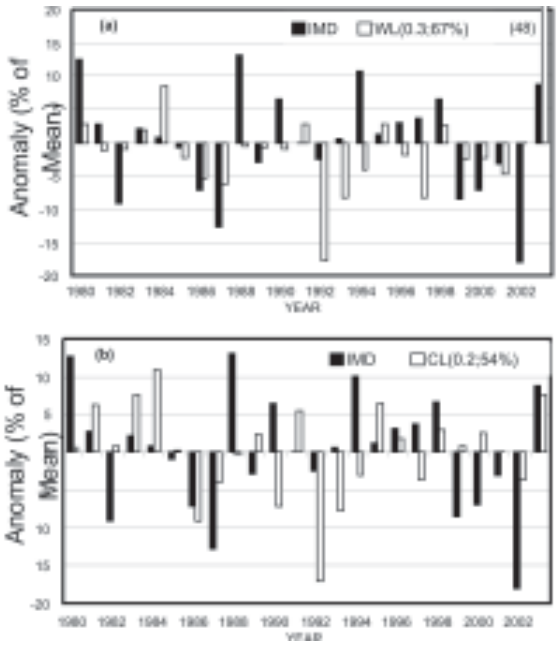


Figue1.17 Inter annual variability in all India seasonal (JJA) rainfall anomaly (as % of respective mean) (a) for WL (top panel) and (b) CL (bottom panel). The two numbers in the bracket in each panel represent, respectively, the correlation coefficient and phase synchronization (%) with observed (IMD) anomalies.

A primary assessment of the comparative skill of the hindcasts from the two ensembles is provided by the IAV in all-India seasonal (JJA) rainfall compared with the corresponding observed variability (expressed as % departure from respective mean) for the two ensembles (Figure 1.17). For WL, the phase synchronization is 16 out of 24 (67%), while the corresponding number for CL is only 13 (54%). Further, the correlation coefficient between the observed and hindcast variability for WL is 0.3, significant above 90% confidence level for the degrees of freedom involved; for CL the correlation coefficient is only 0.2 (Figure 1.17) with significance below 90%.

*K C Gouda and P Goswami*

### B.3 Interannual Variability of Tropical Rainfall Characteristics and the Impact of the Altitude Boost from TRMM PR 3A25 Data

Global and regional interannual variations of rainfall characteristics over the tropics were examined by applying emperical orthogonal function (EOF) analysis to TRMM PR 3A25 data from December 1997 to December 2007. The TRMM PR 3A25 and other TRMM datasets detect the interannual variation of rainfall over the tropics, in concert with the SST change, which is closely related to the El Nino/La Nina cycle, including the pseudo-El Nino periods in 2002 and 2004. In addition we examined the impact of the altitude boost of the TRMM satellite from 350 km to 400 km in August 2001 and found that the boost affects the annual cycle in light rain rate (total, convective and stratiform) A baseline shift occurs in the annual cycle of light convective rain rate (convRainH) with more (less) frequent occurrence before (after) the boost. In contrast, for heavy convRainH, the number events decreases after the boost, especially over land.

*T Nakazawa and K Rajendran*

## C: High Impact Weather Events and variability: Forecasting, Analysis and Observation system Design

### C.1 Numerical Investigations into the Impact of Urbanization on Tropical Mesoscale Events

In recent times there has been increase in the intensity and frequency of heavy rainfall events over the Indian Monsoon region resulting in loss of lives and property in many Indian cities. Increased urbanization, due to altered thermodynamic and mechanical properties of land surface has been known to modulate local weather and trigger high impact weather events like heavy rainfall. Urban heat island effect and increased surface roughness length due to urbanization induce thermal instability, increases mechanical turbulence, and also produce enhanced rainfall downwind of the urban area. Numerical studies have shown that highly urbanized cities are likely to trigger severe convective storms. This study assumes significance in the context of disaster management and mitigation associated with high impact weather events in India.

The fifth generation NCAR /Penn State mesoscale model MM5V3 used in this study (Dudhia et al. 2004) is a mesoscale model with options for parameterization of various processes like cumulus convection, Planetary Boundary Layer (PBL) and radiative forcing. It can support multiple nests with varying horizontal resolution and has non-hydrostatic dynamics.

Three heavy rainfall events have been considered; Mumbai (03UTC, 26th July to 03UTC 27th July 2005), Bangalore (15UTC, 22nd Oct to 15UTC 23rd Oct 2005) and Chennai (06UTC, 26th Oct to 06UTC 27th Oct 2005) over three different locations covering

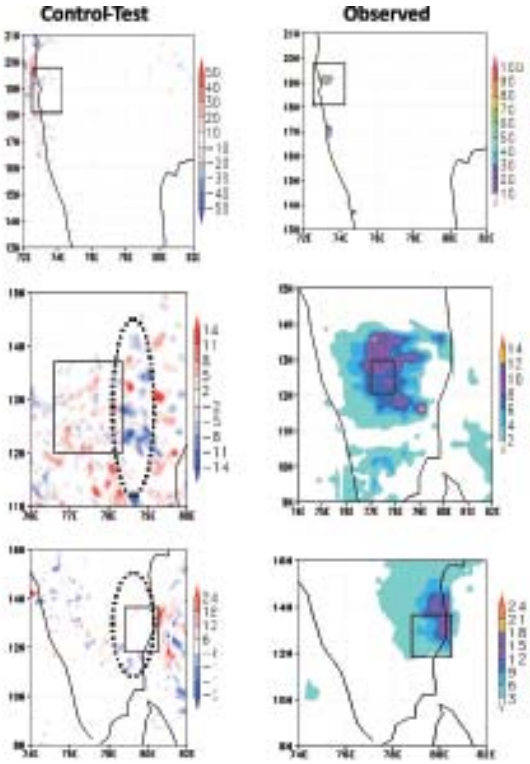


Figure 1.18 Spatial distribution of 24-hour accumulated simulated (left) and observed (right) rain. High intensity spots concentrated around the periphery of urban zone (D3 indicated by boxes) may be seen (around dotted ellipse).

different climatic regions and seasons. The Mumbai event was a very high intensity event that occurred over the west coast of India during the summer monsoon season. The other two events occurred during the winter (north-east monsoon) season; of these, one was over the east coast of India (Chennai 13.5N, 80.17E), while the other was over a continental location (Bangalore 12.59N, 77.35E). The extreme rainfall event that flooded the metropolis of Mumbai on the west coast of India (72.52E and 18.52N) was an intense and highly localized meso-scale convective system, with a spatial scale of only about 30 Kms.

Numerical experiments involve a set of six simulations with control and test simulation for each of the events. Control simulation essentially represents old land use scenario(less urbanized) and test simulations represent modified land surface (current) due to increased urbanization. Only the innermost domain (D3) was modified in all the test runs to reflect the current condition of increased urbanization by modifying land surface properties (surface roughness length, albedo, thermal inertia and moisture availability) with typical urban (50 cm, 18 %, 0.03 cal.cm-2K-1 S-1/2 and 10%) values. In all the experiments, the model was integrated for 3 days starting from 2005-07-25:00 Hour (Mumbai), 2005-10-22:00 (Bangalore) and 2005-10-25:00 (Chennai) respectively.

The results presented above are based on the investigation of three events occurring in different seasons and different geographical locations. All the three events discussed here have shown that urban areas tend to modify the intensity and spatial distribution of rain. In general it was found that total rain (accumulated domain averaged rain) was more in semi-urban or partially urbanized areas (control) than urbanized areas (test). intensification was found to be higher in urban areas with more rain accumulated around the boundary of urban zone or around urban-semi-urban interface zone. Such intensification would eventually contribute to flooding. Urbanization seems to have influenced heavy rainfall events differently over different locations, nevertheless all the events were significantly affected by urbanization.

*S Himesh & P Goswami*

## C.2 Relative Role of Domain Size, Grid Size, and Initial Conditions in the Simulation of High Impact Weather Events

Genesis and evolution of mesoscale events are strongly determined by local inhomogenities of boundary forcings in addition to non-hydrostatic dynamics at small spatial scales. Limited area or mesoscale models

(LAM) thus continue to be the most popular and effective tools for simulating and forecasting mesoscale events. Numerous studies have demonstrated the ability of high resolution mesoscale models to successfully simulate high impact weather events like extreme rainfall and their associated synoptic features. A necessary price for such high horizontal resolution, however, is a small numerical domain of integration due to computational constraints. In reality, both resolution and the size of the mesoscale domains play a critical role in the quality of the simulation. The size of the domain implicitly determines the large-scale dynamics and terrain effects, while the horizontal resolution determines the smallest resolvable scale. The question of relative sensitivity of domain size, horizontal grid distance and initial conditions on the quality of mesoscale simulation, however, has not yet been studied in depth in the context of high impact weather events. The objective of the present study is to investigate this issue in the context of high impact weather event occurred in Indian Monsoon region.

This study is based on an extreme rainfall event that occurred over Mumbai (west coast of India, July 26-27, 2005). The fifth generation NCAR / Penn State mesoscale model (MM5V3) was used with three grid distances (90, 60 30 and 10-km) in our study to examine the relative role of domain size and horizontal grid distance in the simulation of extreme rainfall event. While it could be argued that proper simulation of mesoscale events require much higher grid distance, the focus here is on quantitative assessment of relative roles of domain size versus grid distance through a large number of sensitivity studies. Seven domains (D1 to D7, Figure1.19) of varying longitudinal and latitudinal extents were chosen for this study, out of which five domains (D2 to D6) were common to all the three grid distances (90, 60 and 30km). Domains D1 (90 and 60-km) and D7 (90-km) were considered for only coarser grid distance due to computational constraints. As mentioned above, the larger scales simulated in the model dynamics will depend not only on the size of the domain but also on the geographical coverage. The seven domains were thus chosen to provide an ensemble of large-scale dynamics and terrain effects. For each of the domains, the model was integrated for 5 days starting from five different initial conditions 6-hours apart beginning from 00UTC, 24th July 2005. Although the event was highly localized in both space and time, we have considered a spatial window of $2^{o}x2^{o}$ centered on the general event location and a time window of 24-hour (06UTC, 26th July to 06UTC, 27th July 2005) for diagnosis and analysis.

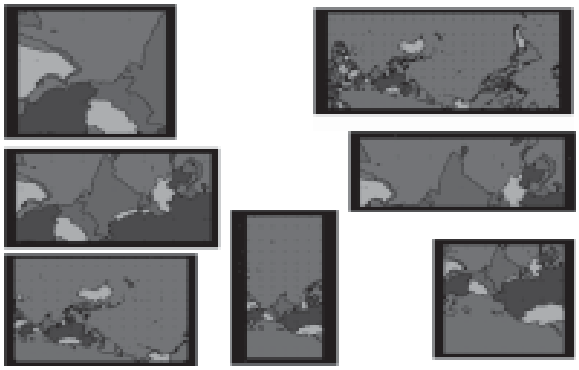

Figure 1.19 Experimental domains.

Comparison of spatial distributions of 24-hour (event window) accumulated, simulated ensemble rainfall based on five initial conditions for five domains of 30-km resolution with satellite data has shown considerable inter-domain variations in the simulated distribution of rainfall. This inter-domain variability in the distribution of rainfall is profound at higher grid spacing. It was also found that the domain D5 (which included equatorial belt) simulated the observed distribution better than all the other domains, and for all the three resolutions. The effects of changes due to longitudinal or latitudinal extents or both on the 24-hour

Table 1.1 Summary of variability of Rav and Rmax in terms of SD as % of mean for different domains, resolution and Initial conditions.

| Rain | Model Domain | Resolution | Initial Condition |
|---|---|---|---|
| $R_{av}$ | 30-40 | 10-30 | 11-50 |
| $R_{max}$ | 34-40 | 21-43 | 6-40 |

accumulated area averaged rainfall (Rav) and the maximum rainfall (Rmax) were analyzed. The results are from ensemble average simulations with the five leads (initial conditions) described above. It was found that changes in the domain size results in significant changes in Rav and Rmax. This variability of Rav and Rmax due to change in domain size and coverage in terms of Standard Deviation (SD) as percentage of mean across different domains was in the range of 30 to 40% and 34 to 40 % respectively. It was seen that effects of change in the domain size in general are larger for lower resolutions. This implies the need for an optimum model configuration with appropriate domain size or ensemble of domains and resolution to resolve both ends of the spectrum of scales. The relative role of resolution on Rav and Rmax was examined. Dispersion of forecasts due to changes in initial conditions provides both a measure of reliability of the forecasts and a measure of variation in mesoscale forecasts due to changes in the large scale conditions (initial fields). In particular, the response to different initial conditions seems to be a strong function of the domain size and geographical coverage as the large scale fields evolve differently over different domains. As a summary of the relative variability or sensitivity of Rav and Rmax in terms of SD (as % mean) with respect to different domains, resolutions and IC's is given in Table.1.1 As another measure of relative sensitivity of the simulations to domain size we have considered standard deviation (as % of mean) in terms of 24-hour accumulated total rain over event location (RT) for different domains (with varying number of domains depending on the resolution). Time evolution of this standard deviation indicated that variation due to change of domain is typically 40 % and can be as much as 70 to 80%; in comparison a change of resolution doesn't change this dispersion that significantly except at isolated hours and not more than by a factor of 2.

*S Himesh and P Goswami*

## C.3 A novel and faster MINRES algorithm for Factor Analysis

Factor analysis (FA) is a popular diagnostic method that reveals associations among a given set of measured parameters. While FA is functionally very similar to the Principal Component Analysis, it is quite different in terms of the underlying assumptions. The composite variables (i.e., factor solutions) derived using FA identify latent variables that explain why measured variables are correlated with each other. However the objective of PCA is to account for the maximum portions of total variance present in a set of measured parameters with a minimum number of composite variables called principal components.

It is also important to consider the assumptions about variance in a data. If parameters are only indicators of a hidden construct to be elucidated or if the error variance represents a significant portion of the total variance, then a more appropriate technique to extract statistical associations among the parameters is FA. Otherwise PCA or FA could lead to similar results. Nevertheless, errors (noise) are an unavoidable part of any measurement. These facts indicate that FA is more apt for estimation of certain coupled modes in a dynamical system, since it emphasizes the co-

variability among noisy variables.

The basic problem in factor analysis is the estimation of a small number m of common factors $f_p$ from a larger number *n* of observed variables $z_j$. This can be stated in a matrix form as

z = Af +Du,

where A is to be estimated. Here **u** represents the errors or unique factors and D their matrix-coefficients. Once a solution has been found, a fundamental theorem of FA states that matrix R of reproduced correlation is given by

$R = AA^T$,

under an assumption of uncorrelated factors (i.e., $f_p$ ). The superscript 'T' indicates transpose of a matrix. The diagonal elements of R are known as communalities. The basic problem is to get a best fit to the observed correlation matrix $R^O$ by the reproduced correlation matrix R. This is achieved by maximally reproducing the off-diagonal elements of $R^O$ in the least square sense: minimize an objective function

$$g(A) = \sum_{j=1}^{n} \sum_{\substack{k=1 \\ k \neq j}}^{n} (r_{jk} - \sum_{p=1}^{m} a_{jp} a_{kp})^2$$

The communalities consistent with this factor matrix (i.e. A) is given by

$$h_j^2 = \sum_{p=1}^{m} a_{jp}^2 \leq 1$$

for j=1,2,….n. In order to have acceptable factor (unrotated) solutions, the minimization of the objective function g(A) is performed under a constraint that communality be less or equal to unity. This method of extraction of unrotated factor solutions is called MINRES (MINimum RESiduals), a term first introduced by Harry Harman. The main advantage of this method is that no assumption about the nature of distribution of data is evoked.

The existing algorithms heavily depend on iterative computations to minimize a certain error-residual, until a global minimum is reached. Hence the time required to find an optimal factor solution increases exponentially with the dimension of the matrix R. Therefore, when this dimension is large, the existing methods may either fail to find an optimal solution or may take enormous computing time. Moreover, theory behind some of the popular algorithms (e.g. Maximum Likelihood ML) assumes that input data is normally distributed. This is not true, in general.

A new faster and simpler method is devised which considerably saves computer time (in orders of magnitude) without compromising the fidelity of factor solutions. It is essential, at this point, to get into the nitty-gritty of the existing FA-algorithms. The numerical iterations in existing methods could be grouped broadly into two categories. Those in the first category, for convenience can be termed as *internal iteration* (II), are associated with matrix computations (viz., inverse, rotation, factorization etc.). The iterations in the second category, called as *external iteration* (EI), are related to dimensionality of a factor-model assumed. Moreover note that the solutions from first part (II) are not robust when the matrix R has a large dimension and/or is ill-conditioned.

The mathematical steps are modified in such a manner that the need for (iterative) matrix computations (in II) is minimized, thereby considerably saving the computer time as well as enhancing the statistical robustness of factor solutions. A numerical code, in Fortran, for this new method is developed and tested successfully for some artificial cases. However, rigorous tests are necessary to examine its full capability as well as its limitations.

***Rameshan Kallummal and A A Lyubushin***